processes

MDPI

Article

Optimized Scheduling of Integrated Energy Systems with Integrated Demand Response and Liquid Carbon Dioxide Storage

Nan Zhang [1], Jie Chen [2,*], Bin Liu [1] and Xiaoning Ji [3]

[1] School of Electrical Engineering, Xinjiang University, Urumqi 830017, China; z_n0725@163.com (N.Z.); liubin19980125@163.com (B.L.)
[2] School of Mechanical Engineering, Xinjiang University, Urumqi 830017, China
[3] Xinjiang Airport (Group) Co., Ltd., Urumqi 830016, China; xj_jxn@163.cn
* Correspondence: chen@xju.edu.cn

Abstract: Energy storage technology can well reduce the impact of large-scale renewable energy access to the grid, and the liquid carbon dioxide storage system has the characteristics of high energy storage density and carries out a variety of energy supply, etc. Therefore, this paper proposes an integrated energy system (IES) containing liquid carbon dioxide storage and further exploits the demand-side regulation potential on the basis of which an integrated demand response model is proposed to consider the cooling, heating, and electricity loads. On this basis, an IES optimal scheduling model with the lowest total system operating cost as the objective function is established, the Yalmip toolbox and Cplex commercial solver are used to solve the algorithms, and the optimal scheduling results are obtained for electricity, heat, and cold under four scenarios, and it is proved through comparative analyses that the model and scheduling strategy established in this paper can optimize the load profile, realize peak shaving and valley filling, and have good economic benefits. Then, by analyzing the impact of the initial pressure of the high-pressure storage tank and fluctuating electricity price on the liquid carbon dioxide energy storage system, the system model established in this paper has good stability. Finally, for the comprehensive demand response model established in this paper, the impact of the demand response of different types of loads on the economy of the system is analyzed in depth from the perspective of economic benefits.

Keywords: integrated energy system; integrated demand response; liquid carbon dioxide energy storage; combined cooling; heating and power (CCHP)

check for updates

Citation: Zhang, N.; Chen, J.; Liu, B.; Ji, X. Optimized Scheduling of Integrated Energy Systems with Integrated Demand Response and Liquid Carbon Dioxide Storage. *Processes* **2024**, *12*, 292. https://doi.org/10.3390/pr12020292

Academic Editor: Peng Li

Received: 28 November 2023
Revised: 16 January 2024
Accepted: 20 January 2024
Published: 29 January 2024

Copyright: © 2024 by the authors. Licensee MDPI, Basel, Switzerland. This article is an open access article distributed under the terms and conditions of the Creative Commons Attribution (CC BY) license (https://creativecommons.org/licenses/by/4.0/).

1. Introduction

Integrated energy systems (IESs) can realize the synergistic development of multiple heterogeneous energy subsystems and complement each other with the advantages of energy gradient utilization and multi-energy joint supply [1]. However, with the increasing proportion of renewable energy penetration, various energy flows are coupled with each other, which poses a serious challenge to the operation and scheduling of IES systems [2].

Energy storage is an indispensable part of the integrated energy system (IES), which can promote clean energy consumption, enhance the economic efficiency of system operation, and also guarantee the reliable supply of various types of loads under the independent operation state of the IES system, which effectively improves the system reliability [3]. Literature [4,5] investigated the effect of some parameters of compressed air energy storage systems on system performance. Li Lexuan et al. [6] established the traditional and advanced models of a supercritical carbon dioxide energy storage system (SC-CCES) from the energy perspective and revealed the influence of device parameters on system performance through the energy loss of each device. Literature [7] proposed a liquid carbon dioxide energy storage (LCES) system based on the Rankine cycle. The system performance of LCES and LAES were comparatively analyzed, and the results showed that LCES has

higher round-trip efficiency and energy efficiency. Wang et al. [8] proposed a new type of liquid carbon dioxide energy storage system to reduce the impact on power system stability due to the level of wind power penetration and compared it with the advanced adiabatic compressed air energy storage system (AA-CAES). The advantages of LCES, such as high energy density and high EVR, have a good potential for storing wind power on a large scale. The above literature only investigates the thermodynamic characteristics of compressed gas energy storage, and the multi-energy cogeneration characteristics of the system are seldom involved. Literature [9] proposes an optimal scheduling model for a cold, hot, and electric microgrid containing a compressed air energy storage system with respect to the temperature characteristics of the compressed air energy storage system. Literature [10] determined the optimal coupling scheme by coupling the liquid compressed carbon dioxide energy storage system with a thermal power unit, which improved the peaking range and flexibility of the thermal power unit. Literature [11] proposed a liquid carbon dioxide energy storage system integrating the transcritical Brayton cycle, electrothermal energy storage, and jet condensation cycle, and the feasibility of the system was verified. Zhu Zhenshan et al. [12] integrated liquid air energy storage into an integrated energy system (IES), taking into account the demand-side response, to realize the economy and low-carbon of the IES from both the demand and supply sides, but only took into account the role of the LCES system in storing electricity. Some scholars [13] also considered the multi-energy supply characteristics of LCES systems but only considered the influence of the key parameters of the energy storage system on the system performance.

With the rapid development of integrated energy systems, the utilization of load-side resources also has a great impact on the consumption of renewable energy, as well as the economic operation of the system, and the demand response strategy has evolved from the demand response of a single load to the integrated demand response (IDR) for multiple types of loads. Literature [14] established a cold–heat–electricity IDR model from the dispatchable value and transmission characteristics of loads. Literature [15] established a framework for electricity and gas energy networks considering IDR, which effectively regulates the balance between the supply and demand of electricity and gas. Zhang Yaoxiang et al. [16] investigated the impact of cold–heat–electricity IDR on the optimal scheduling of the IES system from the multiple time scales within the first day of the week. Literature [17] established an IDR model for electric–thermal loads based on the coupled complementary relationship of electric–thermal loads as well as the elastic response mode of electric loads and the diversity of heat supply modes. Literature [18] took into account the demand side of the user's electricity demand and introduced electric vehicle charging and discharging strategies as a means of guiding the user's electricity behavior. Literature [19] established a two-tier optimization model for a virtual power plant based on demand response, which takes into account the interruptible loads on the user's side, and literature [20] proposed the establishment of the IES low-carbon economic scheduling model with an electricity–gas–heat IDR to optimize the load curve. However, the above studies have only considered the demand response strategies of a single load or two loads and have not conducted an in-depth study on the impacts of a single type and different proportions of load demand response on the economy of the system.

Based on the above background, this paper constructs an optimal scheduling model of IES based on LCES systems from the characteristics of the LCES system's combined cooling, heating, and power supply and, at the same time, implements a demand response strategy for the load side. Firstly, considering the cooling, heating, and electricity load response characteristics, the integrated demand response (IDR) on the user side is divided into price, incentive, and alternative types; then, different system operation scenarios are set up to analyze the impacts of the demand response strategy and the LCES system on the economics and system performance of the IES by comparing the two. Finally, through arithmetic simulation, the effectiveness of the integrated energy system with LCES—considering a verified demand response—and the constructed demand response model are analyzed in depth.

2. Integrated Energy System with LCES

The IES system diagram of this paper is shown in Figure 1, and the new energy generation method adopts photovoltaic unit (PV) and wind turbine (WT) to generate electricity; on the energy conversion side, it mainly includes gas turbine (GT), gas boiler (GB), waste heat boiler (WHB), heat pump (HP), electric chiller (EC), absorption chiller (AC), and LCES storage plant.

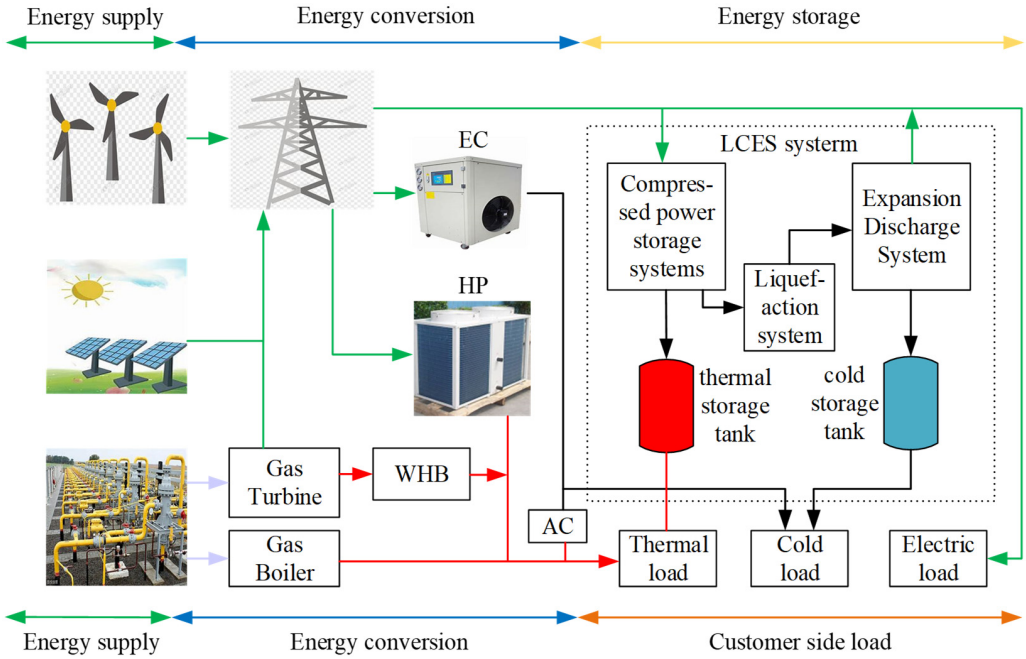


Figure 1. Integrated energy system (IES) structure diagram.

2.1. Renewable Energy Unit Model

Wind power and photovoltaic unit power generation have the advantages of environmental protection and energy saving, but both have great stochasticity, and their mathematical models are as follows:

$$P_{\mathrm{PV},t} = P_{STC} G_{L1}[1 + k(T_c - T_r)]/G_{STC} \tag{1}$$

where $P_{\mathrm{PV},t}$ is the photovoltaic power, unit in kW; P_{STC}, G_{STC}, respectively, are the maximum test power and light intensity under standard test conditions; k indicates the power temperature coefficient; T_c, T_r, respectively, are the panel operating temperature and reference temperature.

$$P_{\mathrm{WT},t} = \begin{cases} 0, v < v_{ci} or v > v_{co} \\ P_r \frac{v - v_{ci}}{v_r - v_{ci}}, v_{ci} < v < v_r \\ P_r, v_r < v < v_{co} \end{cases} \tag{2}$$

where $P_{\mathrm{WT},t}$ is the power generated by the wind turbine; P_r denotes the rated power generated by the wind turbine, unit in kW; v, v_{ci}, v_{co}, v_r denote the actual wind speed, the cut-in wind speed, the cut-out wind speed, and the rated wind speed, respectively, unit in m/s.

2.2. Gas Turbine Model

The gas turbine is capable of converting three forms of energy, electricity, gas, and heat, and is mathematically modeled as:

$$\begin{cases} P_{\mathrm{GT},t} = V_{\mathrm{GT},t} H^{\mathrm{gas}} \eta_{\mathrm{GT}} \\ Q_{\mathrm{GT},t} = P_{\mathrm{GT},t} \eta_L \beta \end{cases} \tag{3}$$

where $P_{GT,t}$ is the electric power output of the gas turbine in time period t; $V_{GT,t}$ is the amount of natural gas consumed by the gas turbine in time period t, unit in m^3; H^{gas} denotes the calorific value of natural gas in KW·h/m^3; η_{GT} and β are the power generation efficiency of the gas turbine and the ratio of thermoelectricity, respectively; $Q_{GT,t}$ is the output thermal power of the gas turbine in time period t, unit in kW; and η_L is the coefficient of waste heat recovery.

2.3. Gas Boiler Model

The gas boiler can realize the balance between the supply and demand of thermal energy of the system with the power output:

$$Q_{GB,t} = V_{GB,t} H^{gas} \eta_{GB} \quad (4)$$

where $Q_{GB,t}$ denotes the output thermal power of the gas boiler in time period t, unit in kW; η_{GB} denotes the efficiency of the gas boiler; and $V_{GB,t}$ denotes the gas intake of the gas boiler in time period t, unit in m^3.

2.4. Absorption Chiller Model

The AC can utilize the heat recovered from the waste heat boiler for refrigeration, and the relationship between the absorbed heat energy and the output cooling power is:

$$L_{AC,t} = COP_{AC} H_{AC,t} \quad (5)$$

where $L_{AC,t}$ is the cooling power generated by the AC at time period t, unit in kW, COP_{AC} denotes the cooling coefficient of the AC, and $H_{AC,t}$ denotes the heat absorbed by the AC at time period t, unit in kW.

2.5. Heat Pump Model

HP can be mathematically modeled by consuming electrical energy to convert heat from low-grade heat energy to high-grade heat energy:

$$Q_{HP,t} = \eta_{HP} P_{HP,t} \quad (6)$$

where $Q_{HP,t}$ is the thermal power output from the heat pump in time period t, unit in kW; η_{HP} is its conversion efficiency; and $P_{HP,t}$ is the electric power consumed in time period t, unit in kW.

2.6. Model of an Electric Chiller

An electric chiller can utilize electrical energy for refrigeration and is mathematically modeled as:

$$L_{EC,t} = COP_{EC} P_{EC,t} \quad (7)$$

where $L_{EC,t}$ indicates the cold power output of EC in time period t, unit in kW, COP_{EC} indicates the refrigeration coefficient of EC, and $P_{EC,t}$ indicates the electric power consumed by EC in time period t, unit in kW.

2.7. Introduction to the LCES Model

The LCES structure is shown in Figure 2. The system consists of a liquid carbon dioxide storage tank, an expander, a compressor, a cooler accumulator, a high- and low-temperature water tank, a heater, a cooler, and a liquefied gasification unit.

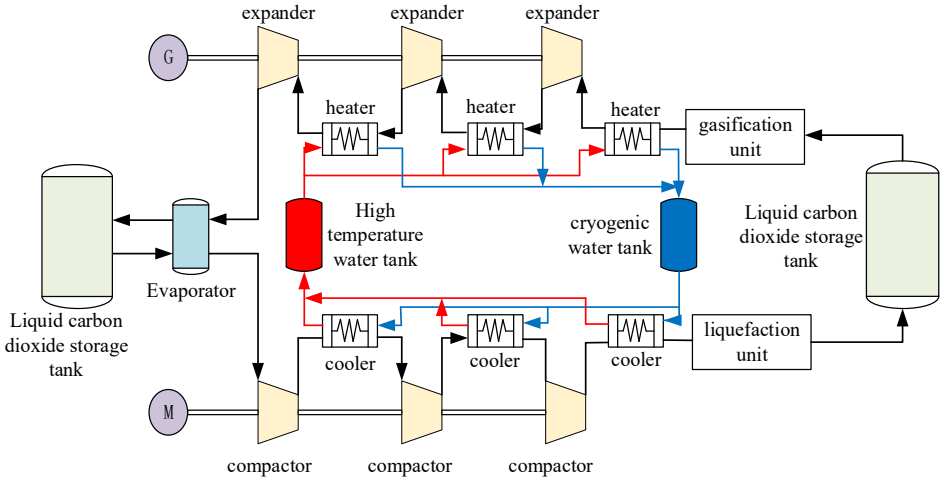


Figure 2. Liquid carbon dioxide energy storage (LCES) system flowchart.

When we need to store energy, liquid carbon dioxide (rich in electricity stored as compression heat from accumulator gasification) will be stored in high-temperature water tanks and go through multi-stage compression to obtain supercritical CO_2. Finally, through the liquefaction device, supercritical CO_2 is stored in high-pressure liquid storage tanks.

When we need to release energy, high-pressure liquid CO_2 is gasified into supercritical CO_2 by a gasification device, multi-stage expansion, and inter-stage heat transfer processes for external power generation, during which the cold energy after heat transfer will be stored in the low-temperature water tank, and finally, the low-pressure gaseous carbon dioxide will be liquefied and stored in the low-pressure liquid tank through the accumulator, to await the next cycle.

When the system is in operation, the compressor and the turbine are the key links in the energy conversion, which are mathematically modeled as follows:

$$\begin{cases} P^{c}_{\mathrm{LCES},t} = \sum\limits_{i=1}^{n_c} \frac{k}{k-1} \frac{m_{c,t} R_{CO_2} T_c^{in}}{\eta_c} \eta_{cs} \left(\beta^{\frac{k-1}{k}} - 1 \right) \\ P^{g}_{\mathrm{LCES},t} = \sum\limits_{i=1}^{n_g} \frac{k}{k-1} m_{g,t} R_{CO_2} \eta_g \eta_{gs} T_g^{in} \left(1 - \lambda^{\frac{k-1}{k}} \right) \end{cases} \tag{8}$$

where $P^{c}_{LCES,t}$ and $P^{g}_{LCES,t}$ are the output power of the compressor and turbine in time period t, unit in kW; $m_{c,t}$ and $m_{g,t}$ are the mass flow rate of CO_2 into the compressor and turbine, unit in kg/s; R_{CO_2} is the gas constant of CO_2, value taken as 189 J/(kg·K); T_c^{in} and T_g^{in} are the inlet temperatures of the compressor and turbine, unit in K; η_{cs} and η_{gs} are the conversion efficiencies of the compressor and turbine; η_c and η_g are the isentropic efficiencies of the compressor and turbine; β is the compression ratio; λ is the expansion ratio; k is the adiabatic index, value taken as 1.4; and n_c and n_g are the number of compressor and turbine stages.

The mathematical models of the LCES system's high-temperature and low-temperature water tanks are:

$$\begin{cases} Q_{h,c} = \sum\limits_{i=1}^{n_c} \left| c_w \dot{m}_{c,t} (T_{c,out,i} - T_{c,in,i}) \right| \\ Q_{c,g} = \sum\limits_{i=1}^{n_c} \left| c_w \dot{m}_{g,t} (T_{g,out,i} - T_0) \right| \end{cases} \tag{9}$$

In the formula, $Q_{h,c}$, $Q_{c,g}$ indicate the heat storage and cold storage, unit in J; c_w is the specific heat capacity of water; $\dot{m}_{c,t}$, $\dot{m}_{g,t}$ are the mass flow rate of water through the heat exchanger, unit in kg/s; $T_{c,out,i}$, $T_{c,in,i}$ are the outlet temperature and inlet temperature of the heat exchanger of the ith level at the time of energy storage; $T_{g,out,i}$, T_0 are the outlet temperature of the heat exchanger of the ith level at the time of discharging and the ambient temperature, unit in K.

3. Integrated Demand Response (IDR) Model for Cooling, Heating, and Electricity

This paper considers the characteristics of an LCES system's combined cooling, heating, and power supply. At the same time, cooling, heating, and power load demands also exist on the user side, which can be managed by integrated demand response (IDR). IDR means that the user side regulates its own energy behavior through price or incentive compensation measures to achieve the purpose of suppressing the load fluctuation, increasing the rate of new energy consumption, and realizing the purpose of shaving peaks and filling valleys. IDR is categorized into price-based, incentive-based, and alternative demand response according to the characteristics of each type of load.

3.1. Price-Based Demand Response Model

When the load type is different, its sensitivity to the electricity price signal is also different. Therefore, the price-based demand response of the electric load is divided into two types of loads that can be cut and shifted, and both types of loads can be adjusted accordingly to the changes in the electricity price. This paper adopts the price elasticity matrix from economics to establish the price demand response model of electric loads, and the price elasticity coefficient is calculated by the following formula:

$$\sigma = \frac{p^0}{\Delta p}\frac{\Delta P_e}{P_e} \tag{10}$$

where Δp and P^0 denote the amount of tariff change and the initial tariff, unit in kW and CNY/(kW·h), respectively; P_e and ΔP_e denote the initial electricity consumption and the amount of electricity change in kW, respectively.

According to the above equation, a matrix containing the self-elasticity coefficient and mutual elasticity coefficient of electricity price changes can be obtained:

$$M = \begin{bmatrix} \sigma_{11} & \sigma_{12} & \cdots & \sigma_{1t} \\ \sigma_{21} & \sigma_{22} & \cdots & \sigma_{2t} \\ \vdots & \vdots & \cdots & \vdots \\ \sigma_{t1} & \sigma_{t2} & \cdots & \sigma_{tt} \end{bmatrix} \tag{11}$$

where σ_{tt} and $\sigma_{mn}(m \neq n)$ denote the self-elasticity and mutual elasticity coefficients of electricity price in time period t in kW, respectively.

Curtailable electric loads decide whether or not to participate in demand response for load curtailment based on the change in the price of electricity before and after the demand response, which can be modeled as follows:

$$\begin{bmatrix} \Delta P_{cut}^1 \\ \Delta P_{cut}^2 \\ \vdots \\ \Delta P_{cut}^t \end{bmatrix} = \begin{bmatrix} P_{cut}^1 & & & \\ & P_{cut}^2 & & \\ & & \ddots & \\ & & & P_{cut}^t \end{bmatrix} M \begin{bmatrix} \frac{\Delta p_1}{p_1^0} \\ \frac{\Delta p_2}{p_2^0} \\ \vdots \\ \frac{\Delta p_t}{p_t^0} \end{bmatrix} \tag{12}$$

where ΔP_{cut}^t and P_{cut}^t denote the amount of curtailable load change and initial curtailable load in time period t in kW, respectively.

Similarly, the transferable electric load can be modeled as follows:

$$\begin{bmatrix} \Delta P_{shift}^1 \\ \Delta P_{shift}^2 \\ \vdots \\ \Delta P_{shift}^t \end{bmatrix} = \begin{bmatrix} P_{shift}^1 & & & \\ & P_{shift}^2 & & \\ & & \ddots & \\ & & & P_{shift}^t \end{bmatrix} M \begin{bmatrix} \frac{\Delta p_1}{p_1^0} \\ \frac{\Delta p_2}{p_2^0} \\ \vdots \\ \frac{\Delta p_t}{p_t^0} \end{bmatrix} \tag{13}$$

where ΔP_{shift}^{t} and P_{shift}^{t} denote the amount of transferable load change and initial transferable load in time period t in kW, respectively.

3.2. Incentive-Based Demand Response Model

Incentive-based demand response means that the agent (or the grid) and the user sign a calling contract; when the user cuts down on the amount of energy used, it can be appropriately compensated to improve the shared energy economy between the two sides. As the human body has a certain degree of fuzzy perception of temperature change, when the heating or cooling temperature changes within a certain range, the human comfort perception changes as well. Therefore, for the hot and cold loads to use incentive compensation measures, taking into account the temperature needs to be within a certain range of change, so the hot and cold demand-type response cuts can be modeled as follows:

$$\begin{cases} \beta_t Y_{cut,\min}(t) \le |Y_{cut}(t)| \le \beta_t Y_{cut,\max}(t) \\ F_{Y,cut} = \sum\limits_{t=1}^{T} [C \cdot |Y_{cut}(t)|]\Delta t \\ Y_{cut}(t) \le 0 \end{cases} \tag{14}$$

where $Y \in \{H, C\}$ indicates one of the hot and cold loads; $Y_{cut}(t)$ indicates the amount of hot and cold load reduction in time period t, and the negative value indicates the reduction, unit in kW; $Y_{cut,\min}(t)$ and $Y_{cut,\max}(t)$ indicate the minimum and maximum reduction of hot and cold loads in time period t in kW, respectively; β_t is the sign of load reduction in time period t, and the reduction occurs when the value is 1; and C is the price of compensation for the reduction of hot and cold loads per unit of power on the user's side, unit in CNY/(kW·h).

3.3. Alternative Demand Response Model

On the IES load side, there is equipment that can use multiple energy sources, so users can choose to use more economical energy sources according to the price comparison of different energy sources, thus improving their energy economy, optimizing the load curve, and, at the same time, realizing peak shaving and valley filling. The mutual conversion of energy sources satisfies the law of conservation of energy, so the alternative demand response for hot and cold loads can be modeled as follows:

$$\begin{cases} \Delta L_t^u = -\lambda_{u,v} \Delta L_t^v \\ \lambda_{u,v} = \frac{\rho_u \omega_u}{\rho_v \omega_u} \end{cases} \tag{15}$$

where $u, v \in \{E, H, C\}$ indicates two of the electric, heat, and cold loads; ΔL_t^u and ΔL_t^v are changes of load u, v in time t in kW, respectively; $\lambda_{u,v}$ is the conversion coefficient between the two loads; ρ and ω indicate the calorific value of the loads and the energy utilization rate.

For this type of demand response, the maximum load switching amount constraint is also considered:

$$\Delta L_{t,\min} \le \Delta L_t \le \Delta L_{t,\max} \tag{16}$$

where $\Delta L_{t,\min}$ and $\Delta L_{t,\max}$ are the minimum and maximum changes in the participating alternative response loads, unit in kW.

4. Optimized Scheduling Model for Integrated Energy Systems with LCES When Considering IDRs

4.1. Objective Function

In this paper, we consider the scheduling strategy with the objective function of minimizing the comprehensive operating cost of the system under the premise of meeting the operating constraints of each unit as well as the constraints of the users' comprehensive

energy satisfaction during the IES operation cycle. In this paper, the scheduling cycle T is 24 h, and 1 h is a scheduling time slot. Then, the objective function is:

$$\min F = F_{buy} + F_{op} + F_{LCES} + F_{com} \tag{17}$$

1. The cost of purchased energy includes the cost of purchased and sold electricity and the cost of purchased gas, as described below:

$$F_{buy} = \sum_{t=1}^{T} \left(\mu_{e,t}^{b} P_{e,t}^{b} - \mu_{e,t}^{s} P_{e,t}^{s} + \mu_{g}^{b} Q_{g,t}^{b} \right) \tag{18}$$

where $\mu_{e,t}^{b}$, $\mu_{e,t}^{s}$ are the purchase price and sale price of electricity at the moment; $P_{e,t}^{b}$, $P_{e,t}^{s}$ are the amount of electricity purchased and sold in the grid at the moment; $Q_{g,t}^{b}$ is the amount of gas purchased at the moment; and μ_{g}^{b} is the price of natural gas.

2. The O&M costs include the operation and maintenance costs of each unit on the supply side and the energy conversion side, as follows:

$$F_{op} = \sum_{t=1}^{T} \varsigma_i P_{i,t} \tag{19}$$

where $i \in \{\mathrm{GB}, \mathrm{GT}, \mathrm{WHB}, \mathrm{AC}, \mathrm{PV}, \mathrm{EC}, \mathrm{ASHP}, \mathrm{WT}\}$, ς_i denotes the unit power O&M cost of the unit, unit in CNY/kW, and $P_{i,t}$ is the unit's output during the time period t in kW.

3. LCES costs are specified below:

$$F_{\mathrm{LCES}} = \sum_{t=1}^{T} \omega_{\mathrm{LCES}} (P_{\mathrm{LCES},t}^{c} + P_{\mathrm{LCES},t}^{g}) \tag{20}$$

where ω_{LCES} is the LCES system O&M cost per unit of power in CNY/kW.

4. Compensation cost means that the agent (or the grid) compensates the user when the user makes appropriate reductions in the amount of energy used by implementing a demand response strategy, as follows:

$$F_{com} = \sum_{t=1}^{T} \sigma_j P_{j,t}^{cut} \tag{21}$$

where $j \in \{H, C\}$, σ_j denote the unit power compensation cost of load j in CNY/kW, and $P_{j,t}^{cut}$ denotes the curtailed power of the j load in time period t in kW.

4.2. Constraints

4.2.1. Renewable Energy Capacity Constraints

The energy supply side takes into account two types of new energy outputs, wind and photovoltaic, which are constrained as:

$$\begin{cases} 0 \le P_{\mathrm{WT},t} \le P_{\mathrm{WT},t}^{\max} \\ 0 \le P_{\mathrm{PV},t} \le P_{\mathrm{PV},t}^{\max} \end{cases} \tag{22}$$

where $P_{\mathrm{WT},t}^{\max}$, $P_{\mathrm{PV},t}^{\max}$ are the maximum outputs of wind turbines and photovoltaic units, respectively, in kW.

4.2.2. Power Balance Constraints

The IES system needs to satisfy all types of energy power balance constraints when operating:

$$\begin{gathered} P_{B,t} - P_{S,t} + P_{\mathrm{WT},t} + P_{\mathrm{PV},t} + P_{\mathrm{GT},t} - P_{\mathrm{ASHP},t} - P_{\mathrm{EC},t} - P^{c}_{\mathrm{LCES},t} + P^{g}_{\mathrm{LCES},t} = P^{0}_{L,t} + P_{cut,t} + P_{shift,t} + \Delta L^{e}_{t} \\ H_{\mathrm{GB},t} + H_{\mathrm{WHB},t} + H_{\mathrm{ASHP},t} - H_{\mathrm{AR},t} + H_{\mathrm{LCES},t} = H^{o}_{L,t} + H_{cut,t} + \Delta L^{h}_{t} \\ C_{\mathrm{AR},t} + C_{\mathrm{EC},t} + C_{\mathrm{LCES},t} = C^{0}_{L,t} + C_{cut,t} + \Delta L^{c}_{t} \end{gathered} \tag{23}$$

where $P_{B,t}$ and $P_{S,t}$ are the amount of electricity purchased and sold from the grid in time period t, respectively; $P^{0}_{L,t}$, $H^{0}_{L,t}$, and $C^{0}_{L,t}$ denote the amount of electricity, heat, and cooling load in time period t before the demand response; all of the above variables are in kW.

4.2.3. Unit Output Constraints

The output of each unit needs to be maintained between its maximum and minimum output, which can be expressed as follows:

$$V^{n,\min}_{m,t} \le V^{n}_{m,t} \le V^{n,\max}_{m,t} \tag{24}$$

where m represents each unit in the IES system; $n \in \{e, h, c\}$ denotes the electric, heat, and cold energy flows, respectively; and $V^{n,\min}_{m,t}$ and $V^{n,\max}_{m,t}$ are the minimum and maximum values of the n-energy outflow of unit m at time period t.

4.2.4. Liquid Carbon Dioxide Energy Storage System Constraints

During the compression energy storage and expansion energy release phases, the output needs to be kept between the maximum and minimum output as follows:

$$\begin{cases} P^{c,\min}_{\mathrm{LCES},t} v_{c,t} \le P^{c}_{\mathrm{LCES},t} \le P^{c,\max}_{\mathrm{LCES},t} v_{c,t} \\ P^{g,\min}_{\mathrm{LCES},t} v_{g,t} \le P^{g}_{\mathrm{LCES},t} \le P^{g,\max}_{\mathrm{LCES},t} v_{g,t} \end{cases} \tag{25}$$

Unit start–stop constraints:

$$v_{c,t} + v_{g,t} \le 1 \tag{26}$$

where $P^{c,\min}_{\mathrm{LCES},t}$, $P^{c,\max}_{\mathrm{LCES},t}$, $P^{g,\min}_{\mathrm{LCES},t}$, and $P^{g,\max}_{\mathrm{LCES},t}$ are the minimum and maximum output power in the compression and expansion phases, respectively, in kW; $v_{c,t}$ and $v_{g,t}$ are the start–stop flags of the unit, which are 0–1 variables.

4.2.5. Customer Satisfaction Constraints on Electricity Use

The user's energy satisfaction needs to be taken into account when implementing the demand response strategy, and, in this paper, only the satisfaction of electricity consumption is considered, which can be defined as follows:

$$s = 1 - \frac{\sum_{t=1}^{T} \left| P^{0}_{L,t} + P_{cut,t} + P_{shift,t} + \Delta L^{e}_{t} \right|}{\sum_{t=1}^{T} P^{0}_{L,t}} \tag{27}$$

Then, there is $s \ge s_{\min}$, where s and $s_{\min}$ are customer satisfaction with electricity and satisfaction minimum.

4.2.6. Model Solving Methods

In this paper, the IES optimal scheduling model is developed based on the mathematical model of each device in the system, which is a mixed integer linear programming (MILP) problem and, therefore, is solved using the YALMIP/CPLEX toolbox in Matlab (R2022a).

5. Calculated Case Analysis

5.1. Calculation of the Basic Conditions

This paper involves cold, heat, electricity, wind power, and photovoltaic power, which are analyzed with data from an industrial park in Northwest China as a reference. The

selected scheduling period is 24 h, and the unit scheduling time is 1 h. The forecasted electricity, heat, and cold loads, as well as the forecasted wind and photovoltaic unit power, are shown in Figure 3.

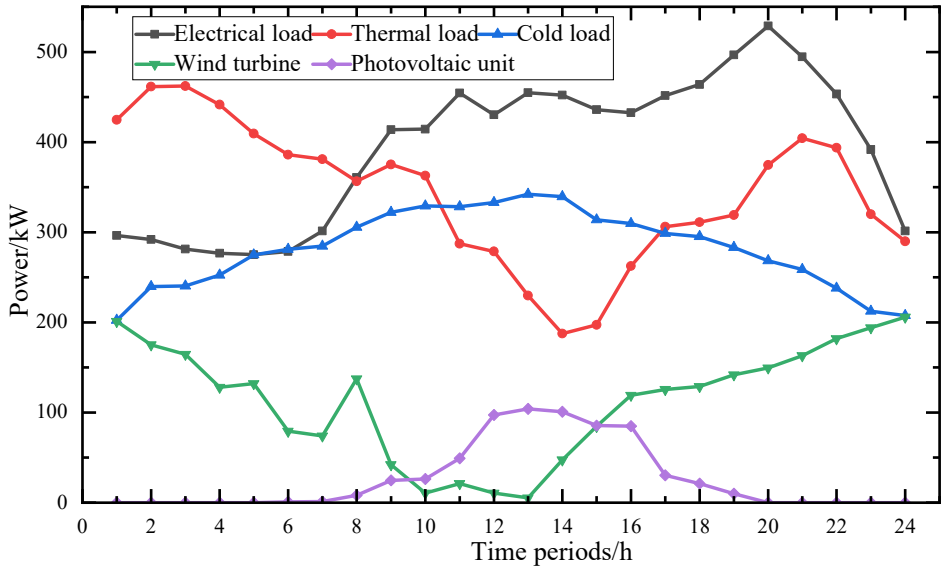


Figure 3. Forecasts of cooling, heating, and electrical loads and wind and photovoltaic outputs.

The main equipment parameters of the integrated energy system (IES) and the LCES system are shown in Table 1. In this paper, the time-sharing tariff strategy is used. The specific price is shown in Table 2, the relevant elasticity coefficients in the price elasticity matrix are shown in Table 3, and the relevant equipment parameters of the IES system are shown in Table 4.

Table 1. Liquid carbon dioxide energy storage (LCES) system's main equipment parameters.

Project Title	Value	Project Title	Value
Compressor Stages	3	Turbine stages	3
Compressor isentropic efficiency	0.85	Turbine isentropic efficiency	0.85
Mechanical efficiency of compressors	0.9	Mechanical efficiency of turbines	0.9
Compression ratio	4	Expansion ratio	3.7
Compression power range /kW	10–100	Expansion power range /kW	10–100
Initial tank pressure /kPa	4500–5500	Environmental pressure /MPa	0.1

Table 2. Tou electricity price (CNY/kW·h).

Project Title	Time Period	Price
Peak hour	10:00–15:00, 17:00–21:00	1.35
Usual hour	7:00–10:00, 21:00–22:00,15:00–17:00	0.87
Valley hour	22:00–next day 07:00	0.4

Table 3. Coefficient of price elasticity of demand.

	Peak Hour	Usual Hour	Valley Hour
Peak hour	−0.1	0.016	0.012
Usual hour	0.016	−0.1	0.01
Valley hour	0.012	0.01	−0.1

Table 4. Other equipment parameters of the integrated energy system (IES).

Parameter	Value	Parameter	Value
η_{GT}	0.35	$P_{GT,max}$/kW	300
η_{GB}	0.90	$Q_{GB,max}$/kW	300
COP_{AC}	1.00	$L_{AC,max}$/kW	150
η_{HP}	4.00	$Q_{HP,max}$/kW	150
COP_{EC}	3.50	$L_{EC,max}$/kW	300

5.2. Analysis of Example Results

5.2.1. Analysis of Economic Benefits

Considering that the selected equipment parameters and load data, as well as the system structure in the IES system, differ from the existing research results and are not highly comparable with each other, in order to compare the impacts of the LCES system and the demand response strategy on the IES system, this paper sets up the following four scenarios for comparative analysis:

- Scenario 1: LCES system is not included, and demand response is not considered;
- Scenario 2: including only the LCES system;
- Scenario 3: Considering only demand response;
- Scenario 4: Both LCES system and demand response are considered.

In each of the above scenarios, the parameters of each device are kept consistent. The dispatch operation cost of each scenario is shown in Table 5, from which it can be seen that the cost of purchased energy is the main factor affecting the total operation cost of the system, which is due to the fact that the integrated energy system selected in this paper needs to purchase a large amount of energy from the higher-level grids and gas grids. Comparing the four scenarios set up, although the operation cost of Scenario 2 increases by CNY 252.2 after adding the LCES system, its purchased energy cost and total operation cost decrease by CNY 443.8 and CNY 191.6, respectively, which is attributed to the fact that the LCES system can store the system's excess power and release it when needed, reducing the waste of energy. In Scenario 3, after the demand response strategy is implemented, during the high tariff hours, the customer reduces their electricity consumption during the peak hours to reduce the cost and increases their electricity consumption during the low tariff hours, which reduces the cost of system operation. Scenario 4 considers both the demand response strategy and the incorporation of the LCES system, and it can be seen that the energy purchase cost and the total system operation cost are reduced by CNY 1148 and CNY 881.7, respectively, compared with Scenario 1 and the economic benefits brought about are more significant.

Table 5. System operating costs for each scenario.

Scenario	Cost of Energy Purchases	Operation and Maintenance Costs	Demand Compensation Costs	Total Cost/(CNY)
Scenario 1	5380.4	963.5	0	6343.9
Scenario 2	4936.6	1215.7	0	6152.3
Scenario 3	4642.9	948.5	29.7	5621.1
Scenario 4	4232.4	1200.1	29.7	5462.2

5.2.2. Analysis of Dispatching Results

After the implementation of the demand response strategy, the electric load optimization curve of the system is shown in Figure 4, from which it can be seen that the original electric load has an obvious peak and valley distribution. During high tariff hours, price-based demand response can transfer part of the load to low tariff hours, and users can also choose to cut part of the electric load during high tariff hours. Substitution-based demand response can replace part of the electric load during high tariff hours with cold and hot

loads, and electric loads can be used during low tariff hours at night to replace cold and hot loads. This optimizes the load curve and achieves peak shaving and valley filling.

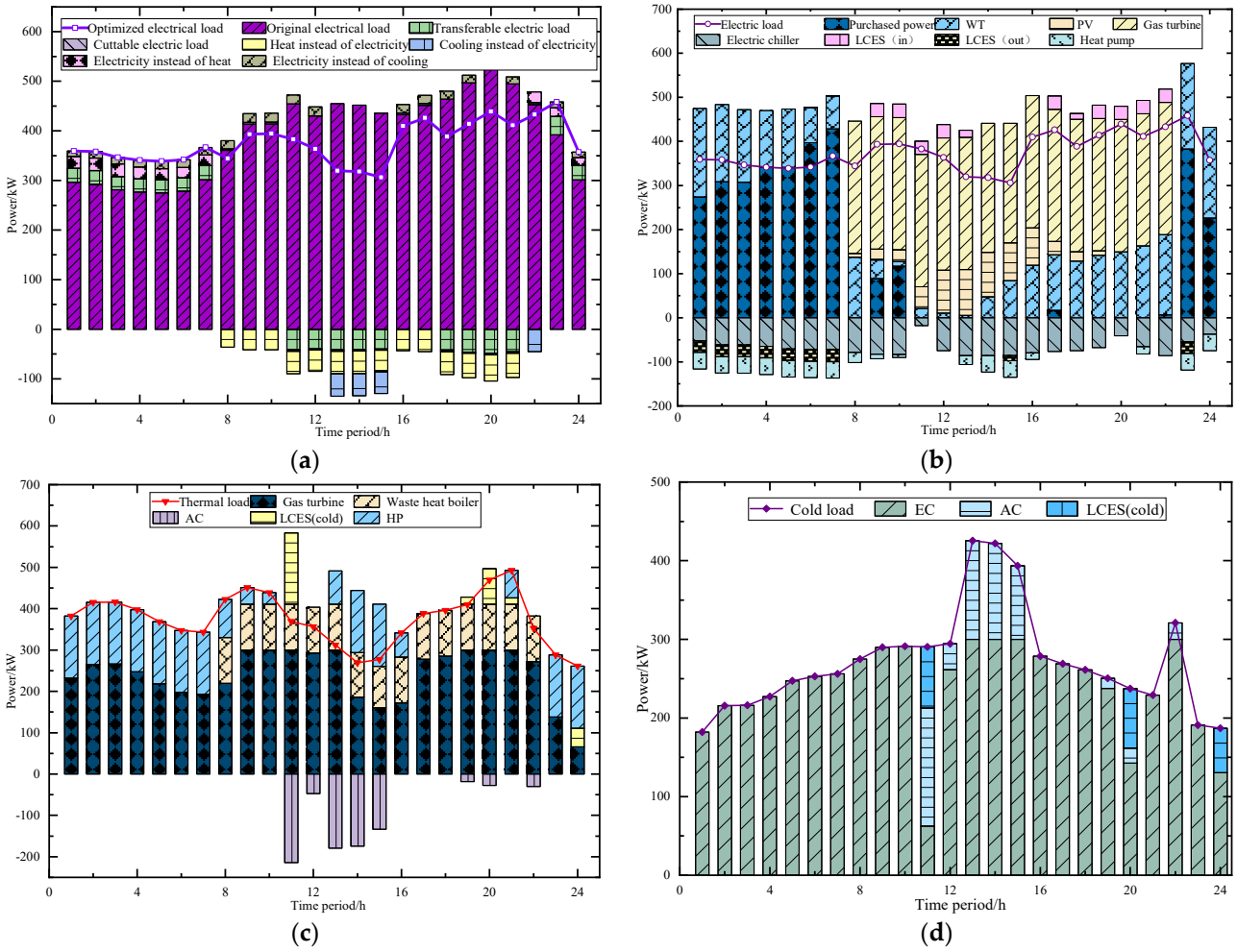


Figure 4. Arithmetic scheduling results. (**a**) Integrated demand response (IDR) of customer-side electric load distribution. (**b**) Electric load supply–demand balance. (**c**) Heat load supply–demand balance. (**d**) Cold load supply–demand balance.

The gas, cooling, and heat required by the IES system are mainly satisfied by purchasing from the higher level. For the power demand of the system, priority is given to the consumption of WT and PV outlets, and during the nighttime low tariff hours (22:00–next day 07:00), the system meets the power demand by purchasing a large amount of power from the higher level. During this period, the EC and HP consume some of the power to satisfy the users' cooling and heating power demand. In the higher tariff period (07:00–22:00), the system purchases less power from the higher level, and gas turbine and new energy outputs are used to satisfy most of the user-side power demand because the tariff is higher in this period, while the unit operation cost is relatively low, which ensures the system's operation economy. At the same time, the heat pump output is lowered, and the waste heat boiler and absorption chiller also make full use of the heat generated by GT to meet the demand for heating and cooling energy on the user side.

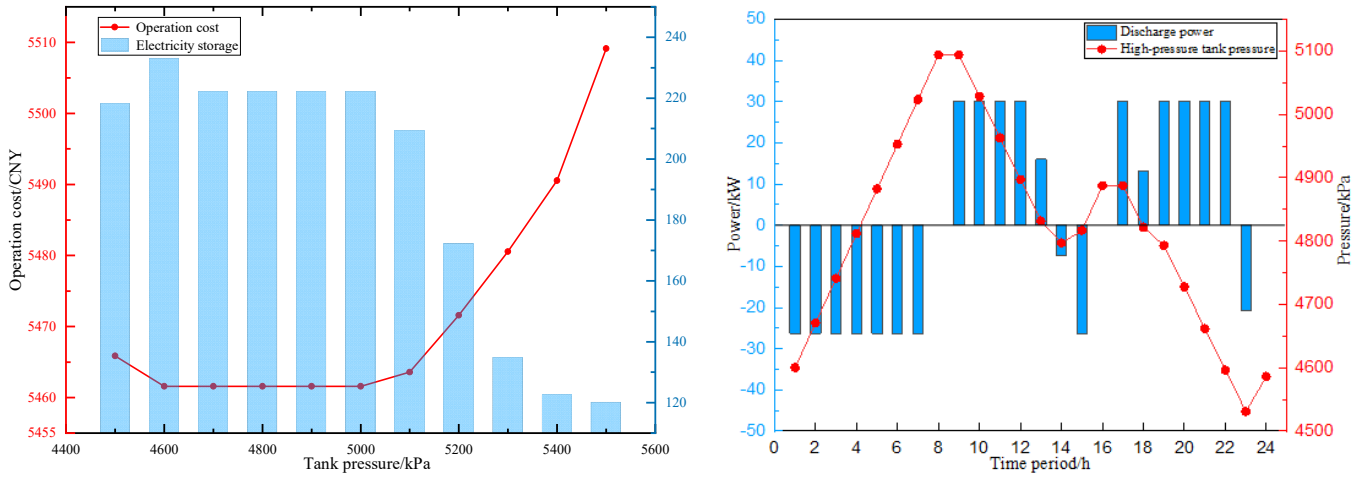
For the supply and storage characteristics of the LCES system, it can be seen from Figure 4b that the LCES system can store the excess power of the system during the nighttime when the electricity price is low and the load is low and release the stored power for the use of the system when the electricity price is high to improve the operation economy of the system. In terms of cooling and heating output, the cooling and heating storage tanks in the LCES system can work together with other cooling and heating equipment to

ensure that the user side of the cooling and heating power demand. It can be seen that the LCES system has a good ability to supply multiple types of energy.

5.2.3. Initial Pressure Sensitivity Analysis of LCES High-Pressure Storage Tanks

The liquid carbon dioxide energy storage system is a complex multi-energy system. The system operation contains multiple energy conversion and transfer links, so the parameter design of the LCES system has a certain impact on the operational performance of the IES system. This paper analyzes the impact of the initial pressure of the supercritical storage tank of the LCES system on the operating cost of the system.

As shown in Figure 5a, within the initial pressure range of the storage tank set in this paper, when the initial pressure of the high-pressure storage tank in the LCES system changes, it has an impact on the operating cost and power storage of the IES system. When the initial pressure is greater than 5000 kPa, the operating cost of the system increases significantly; on the contrary, the power storage of the system decreases, and when the initial pressure of the tank is 4600 kPa, the operating cost is lower, and the power storage is higher. When the initial pressure of the storage tank is 4600 kPa, its operating cost is lower, and its power storage is higher. This is because when the initial pressure increases, it will increase the compressor inlet pressure to reduce the compressor pressure ratio, thus reducing the energy storage stage of the unit of mass compression power consumption. Meanwhile, the expander outlet pressure also increases, and the expansion ratio decreases, resulting in a reduction of the unit of mass work done by the other energy supply units in the IES to increase the output system's operating costs.



(**a**) (**b**)

Figure 5. (**a**) Effect of initial pressure of CO_2 high-pressure storage tanks on system performance. (**b**) Relationship between LCES charging and discharging energy and pressure of high-pressure storage tank.

Figure 5b reflects the relationship between the charging and discharging processes of the LCES system and the pressure change of the system's high-pressure storage tank, which verifies the correctness of the model built in this paper.

5.2.4. Sensitivity Analysis of IES Operating Costs to Electricity Prices

When the electricity price fluctuates within a certain range, the total operating cost of the IES system also changes. Figure 6 shows the relationship between the operating costs of the four scenarios studied in this paper and the fluctuation of the electricity price when the electricity price changes, with 0% being the original parameter, i.e., the rate of change when the electricity price does not fluctuate. As can be seen in Figure 6, when the electricity price decreases or increases, the operating cost of each scenario decreases and increases. Comparing Scenarios 1, 2, 3, and 4, it can be seen that when demand response

curation or an LCES system is added to the system, the total cost of IES operation fluctuates with the fluctuating electricity price, and the rate of change fluctuates less than scenario 1, which means that the fluctuation of the system operation cost in Scenarios 2, 3, and 4 is smaller. Scenario 3 fluctuates less than Scenario 1 because the demand response strategy can replace part of the electric loads with cooling and heating loads, and Scenarios 2 and 4 fluctuate even less because the system in Scenarios 1 and 3 does not have the function of energy storage (such as electric chillers and heat pumps), and thus, is not able to cope with fluctuations in the operating costs of electric equipment with the fluctuation of the electricity price.

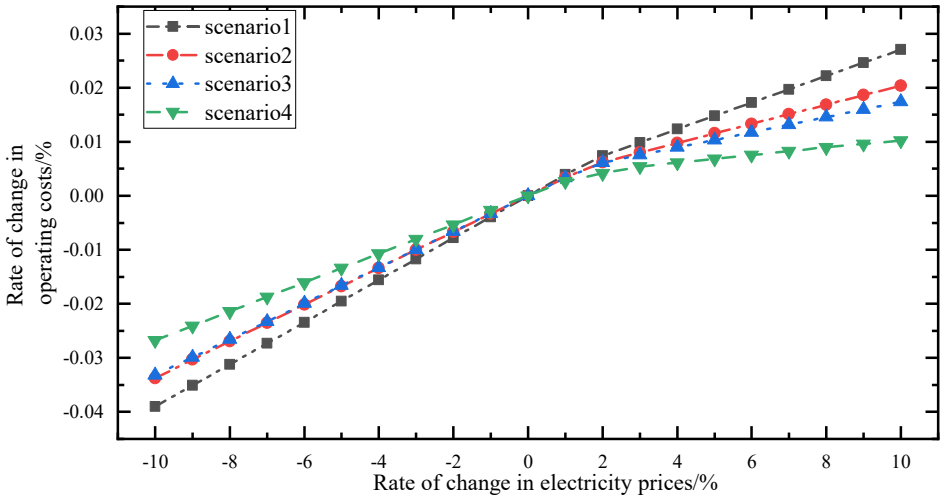


Figure 6. Changes in the cost of four scenarios when electricity prices fluctuate.

5.2.5. Influence of Cold–Heat–Electric Load IDR on IES Operation Economics

In the integrated energy system operation, in order to ensure the dynamic balance of supply and demand, we should prioritize the demand response of the load side in order to study the impact of the demand response of different types of loads on the economics of IES operation. Table 6 shows the results of the following seven scenarios.

Table 6. Impact of different integrated demand responses (IDRs) on integrated energy system (IES) operating economics.

Scenario	IES Running Costs/CNY
R1: Considering only electrical load DR	5858.60
R2: Considering only thermal loads DR	6282.58
R3: Considering only the cooling load DR	6277.62
R4: Considering only electrical and thermal loads IDR	5898.74
R5: Considering only electrical and cooling loads IDR	5894.38
R6: Considering only cooling and heating loads IDR	6274.32
R7: Considering cooling, heating, and electrical loads IDR	5517.54

Comparing scenario R1 with scenarios R2 and R3, it can be seen that the operating cost of the IES system is reduced by 6.75% and 6.67%, respectively. The reduction of the operating cost is greater when only the electric load demand response is considered. The analysis of the seven scenarios can be analyzed in a comprehensive manner to show that the operating cost of the system, in general, decreases by a larger magnitude when the electric load demand response is added, and it can be learned that the impact of the electric load DR has a greater impact on the economy of the system than the impact of the other types of load demand response. In order to gain a deeper understanding of the impact of electric load DR on the economics of IES, the sensitivity of the IES system is also analyzed for the various types of electric load DR scenarios with different weights, as shown in the

figure, with a weight change step of 10%, and a range of change between ±100% of the original preset value.

As shown in Figure 7 that the operating cost of the IES system gradually decreases as the DR weights of different types of electric loads increase. The change of the curtailable class of electric loads has a negligible impact on the cost, while the transferable and substitutable electric loads have a great impact on the cost because the transferable loads are shifted from the time when the price of electricity is high to the time when the price of electricity is low, and the substitutable class of electric loads is replaced by the high price of electricity. At the same time, the new energy output tends to be larger in the low electricity price period. Load transfer and substitution measures can improve the new energy power generation on-line level and reduce the new energy output and load side of the peak and valley staggered impact. The analysis shows that by setting the appropriate proportion of electric load, DR can better play the role of time-sharing tariff guiding mechanism and improve the operating economy of the system.

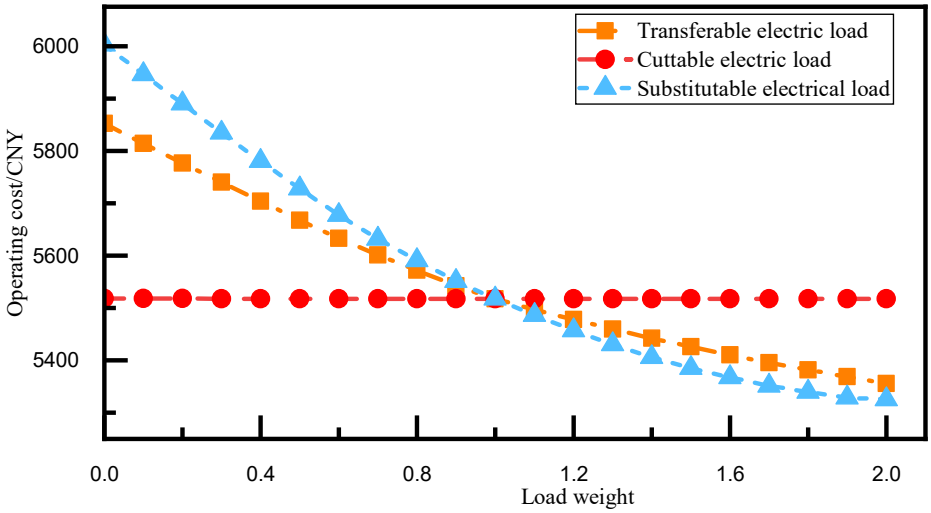


Figure 7. Impact of electric load demand response(DR) weights on integrated energy system (IES) operating costs.

6. Conclusions

This paper proposes an optimal scheduling model of the integrated energy system with liquid carbon dioxide energy storage (LCES), incorporates an integrated demand response (IDR) strategy into the scheduling process, analyzes the calculation examples, and finds that the scheduling strategy in this paper reduces the operating cost by 13.9% compared to the case where LCES and IDR are not considered. Similarly, the cost of considering LCES and IDR at the same time is 11.2% and 2.8% lower than the case where LCES and IDR are considered individually, 11.2% and 2.8%, respectively. Then, the changes in the system operating costs in different scenarios when the initial pressure of the LCES high-pressure storage tanks and the electricity price change are analyzed; finally, the demand response model developed in this paper is analyzed in depth, and the following conclusions can be obtained by comparing the dispatch results of different scenarios:

- The optimization strategy proposed in this paper fully exploits the regulation potential of the user-side response and the participation of the LCES system in the system scheduling, promotes the multi-energy complementary operation of the system, and realizes the cogeneration characteristics of cooling, heating, and power while achieving the flexible operation of the IES.
- The working mode LCES system has good multi-energy cogeneration characteristics, and after participating in the system operation, it effectively reduces the operating cost of the system and also promotes the level of new energy consumption.

- The initial pressure of the supercritical storage tank of the LCES system has a certain impact on the system performance, and within a certain range, it has no significant impact on the operating cost of the system.
- When the LCES system is added to the IES system and demand response is considered, the system operating cost is more stable when the price of electricity fluctuates, and it is more economically efficient than the traditional IES system.
- The DR of transferable and curtailable electric loads has a greater impact on the level of system economics.

In this paper, the multi-energy supply characteristics of a liquid carbon dioxide energy storage system are taken into account. However, the influence of the LCES system parameters on the operating characteristics of the IES system is not considered in the operation schedule, and the influence of the capacity configuration of each energy supply device in the integrated energy system on the operation scheduling of the system is also not considered. The influence of the parameters of the LCES system will be investigated in depth in the future, and the intelligent optimization algorithm will be added to the system to carry out the capacity configuration of the various energy supply devices.

Author Contributions: Conceptualization and methodology, N.Z.; simulation and analysis, N.Z.; investigation, N.Z.; data curation, N.Z.; writing—original draft preparation, N.Z.; writing—review and editing, N.Z.; supervision, J.C., B.L. and X.J.; literature research, N.Z. All authors have read and agreed to the published version of the manuscript.

Funding: This research was funded by Major science and technology projects of Xinjiang Uygur Autonomous Region, grant number 2022A1001-3.

Data Availability Statement: Data are contained within the article.

Acknowledgments: I am immensely thankful to Jie Chen for her patient guidance throughout the development of this paper. I am deeply appreciative of Bin Liu and Xiaoning Ji for their supervision while I was writing my dissertation. I am also deeply appreciative of Jie Chen for accepting my participation in this pivotal project and providing me with this invaluable opportunity. Once more, I wish to convey my heartfelt gratitude to both of these mentors!

Conflicts of Interest: Author Xiaoning Ji was employed by the company Xinjiang Airport (Group) Co. The remaining authors declare that the research was conducted in the absence of any commercial or financial relationships that could be construed as a potential conflict of interest.

Abbreviations

IES	Integrated energy system
SC-CCES	Supercritical carbon dioxide energy storage
LCES	Liquid carbon dioxide energy storage
AA-CAES	Advanced adiabatic compressed air energy storage
DR	Demand response
IDR	Integrated demand response
PV	Photovoltaic
WT	Wind turbine
GT	Gas turbine
GB	Gas boiler
WHB	Waste heat boiler
AC	Absorption chiller
HP	Heat pump
CCHP	Combined cooling, heating, and power

References

1. Li, J.; Zhu, M.; Lu, Y. An Overview of Optimized Scheduling of Integrated Energy Systems. *Power Syst. Technol.* **2021**, *45*, 2256–2272.
2. Yan, Y.; Zhang, C.; Li, K. Optimized Operation Strategy of Cogeneration Microgrid with Compressed Air Energy Storage. *Proc. CSEE* **2018**, *38*, 6924–6936+7126.
3. Qu, J.; Zhu, L.; Liu, Z.; Hou, K. Reliability Assessment for Integrated Energy Microgrid System with Compressed Air Energy Storage. *J. Northeast Electr. Power Univ.* **2022**, *42*, 8–18+105.
4. Arabkoohsar, A.; Rahrabi, H.R.; Alsagri, A.S.; Alrobaian, A.A. Impact of Off-design operation on the effectiveness of a low-temperature compressed air energy storage system. *Energy* **2020**, *197*, 117176. [CrossRef]
5. Rahbari, H.R.; Arabkoohsar, A. A thorough investigation of the impacts of trigeneration-CAES off-design operation on its thermodynamics, economic and environmental effectiveness. *Sustain. Energy Technol. Assess.* **2021**, *44*, 101024. [CrossRef]
6. Li, L.; Xu, Y.; Guo, H.; Zhang, X.; Chen, H.; Zhou, X. Exergy destruction characteristics of a supercritical carbon-dioxide energy storage system. *Energy Storage Sci. Technol.* **2021**, *10*, 1824–1834.
7. Xu, M.; Zhao, P.; Huo, Y.; Han, J.; Wang, J.; Dai, Y. Thermodynamic analysis of a novel liquid carbon dioxide energy storage system and comparison to a liquid air energy storage system. *J. Clean. Prod.* **2020**, *242*, 118437. [CrossRef]
8. Wang, M.; Zhao, P.; Wu, Y.; Dai, Y. Performance analysis of a novel energy storage system based on liquid carbon dioxide. *Appl. Therm. Eng.* **2015**, *91*, 812–823. [CrossRef]
9. Ghazvini, A.; Sedighizadeh, M.; Olamaei, J. Semidefinite programing as a tool for economic-environmental operation of a microgrid including compressed air energy storage and electric vehicle. *J. Energy Storage* **2021**, *43*, 103215. [CrossRef]
10. Yan, X.; Wang, X.; Han, X.; Han, Z. Study on coupling scheme of liquid compressed carbon dioxide energy storage system and thermal power unit. *Therm. Power Gener.* **2023**, *52*, 90–100.
11. Liu, Z.; Liu, Z.; Xin, X.; Yang, X. Proposal and assessment of a novel carbon dioxide energy storage system with electrical thermal storage and ejector condensing cycle: Energy and exergy analysis. *Appl. Energy* **2020**, *269*, 115067. [CrossRef]
12. Zhu, Z.; Sheng, M.; Chen, Z. Low-carbon economic dispatching of integrated energy system considering liquid air energy storage and integrated demand response. *Electr. Power Autom. Equip.* **2022**, *42*, 1–8.
13. Ran, P.; Zhang, S.; Wang, Y.; Li, Z.; Zhao, G. Research on the Characteristics of Combined Cooling, Heating and Power System with Compressed Air Energy Storage Coupled with Supercritical Carbon Dioxide Brayton Cycle. *J. Chin. Soc. Power Eng.* **2022**, *42*, 1077–1088.
14. Wang, J.; Ren, Y.; Guo, Z.; Zhang, Y. Optimal scheduling of integrated energy system considering integrated demand response and reward and punishment ladder carbon trading. *Energy Storage Sci. Technol.* **2022**, *11*, 2177–2187.
15. Sheikhi, A.; Bahrami, S.; Ranjbar, A.M. An autonomous demand response program for electricity and natural gas networks in smart energy hubs. *Energy* **2015**, *89*, 490–499. [CrossRef]
16. Zhang, Y.; Liu, W.; Pang, Q.; Li, Y.; An, N.; Li, F. Multi-Timescale Trading Strategies for the Participation of Multi-Energy Demand Response in the Consumption of Blocked New Energy Sources. *Electr. Power Constr.* **2023**, *44*, 1–11.
17. Wang, Y.; Ma, Y.; Song, F.; Ma, Y.; Qi, C.; Huang, F.; Xing, J.; Zhang, F. Economic and efficient multi-objective operation optimization of integrated energy system considering electro-thermal demand response. *Energy* **2020**, *205*, 118022. [CrossRef]
18. Tan, Y.; Zhi, Y.; Luo, Z.; Fan, H.; Wan, J.; Zhang, T. Optimal Scheduling of Virtual Power Plant with Flexibility Margin Considering Demand Response and Uncertainties. *Energies* **2023**, *16*, 5833. [CrossRef]
19. Cui, H.; Li, F.; Hu, Q.; Bai, L.; Fang, X. Day-ahead coordinated operation of utility-scale electricity and natural gas networks considering demand response based virtual power plants. *Appl. Energy* **2016**, *176*, 183–195. [CrossRef]
20. Yun, B.; Zhang, E.; Zhang, G.; Ma, K.; Zhang, B. Optimal operation of an integrated energy system considering integrated demand response and a "dual carbon" mechanism. *Power Syst. Prot. Control* **2022**, *50*, 11–19.

Disclaimer/Publisher's Note: The statements, opinions and data contained in all publications are solely those of the individual author(s) and contributor(s) and not of MDPI and/or the editor(s). MDPI and/or the editor(s) disclaim responsibility for any injury to people or property resulting from any ideas, methods, instructions or products referred to in the content.